**Title**: A New Developmental Mechanism for the Separation of the Mammalian Middle Ear Ossicles from the Jaw

**Journal**: *Proceedings of the Royal Society B: Biological Sciences*

**Authors:** Daniel J. Urban[1†], Neal Anthwal[3†], Zhe-Xi Luo[4], Jennifer A. Maier[1], Alexa Sadier[1], Abigail S. Tucker[3], and Karen E. Sears[1,2*]

**Affiliations:**

[1]School of Integrative Biology, 505 S Goodwin Avenue, University of Illinois, Urbana IL 61801 USA

[2] Carl Woese Institute for Genomic Biology, 1206 W Gregory Drive, University of Illinois, Urbana IL 61801 USA

[3]Department of Craniofacial Development and Stem Cell Biology, King's College London, London, UK

[3]Department of Organismal Biology and Anatomy, University of Chicago, Chicago IL 60637 USA

[†]These authors contributed equally to this work.

**Correspondence to**: Dr. Karen Sears, ksears2@illinois.edu

**Article DOI**: 10.1098/rspb.2016.2416

**Supplementary Materials and Methods:**

**Immunofluorescence.** In preparation for cryosectioning, specimens were rehydrated through a reverse MeOH series and rinsed in 1xPBS for 1.5 hours (with changes every 30 minutes). Afterward, they were sunk in 30% sucrose solution (in 1xPBS) and stored at 4 degrees C overnight. The following day, specimens were equilibrated in Optimal Cutting Temperature compound (OCT) at room temperature for 1-3 hours. Finally, they were transferred into a mold with fresh OCT and flash frozen in a mixture of dry ice and ethanol (EtOH). Frozen blocks were stored in -80 degrees C until cut. Specimens were sectioned in a Thermo Scientific Cryostat Microtom (Microm HM550) at a thickness of 10 microns. Sections were collected on superfrost glass slides and immediately stored on dry ice until transferred to a -20 degree freezer.

Sections from 16, 18, and 20 day opossums underwent immunofluorescence (IF) staining in order to highlight apoptosis, autophagy, and cellular proliferation (32, 33). IF protocol for cellular proliferation (using Phosphohistone H3 (Ser10) antibody from Cell Signaling Technology) and autophagy (using Anit-LC3B antibody (ab51520) from Abcam). Day 1 of protocol: blocking buffer (100mL 1xPBS + 1mL HIGS + 100ul Triton X-100), block for 10 min, gently dry, 100ul per slide phH3 1:100 concentration (100ul buffer + 1ul phH3) or LC3B at 1:1000 concentration (1mL buffer + 1ul LC3B), cover slip, humidified chamber in 4 degree C overnight (with excess buffer). Day 2 of protocol: 3x 20 washes with blocking buffer, 100ul secondary antibody per slide 1:250 concentration (300ul buffer + 1.2ul Goat anti-Rabbit (Alexa Fluor 488 conjugate from Invitrogen)), cover slip, humidified chamber at room temp for 1 hour (in the dark), 3x 20 min washes in buffer (keep in dark), gently dry, 2-3 drops Vectashield Mounting Medium with DAPI, store at 4 degrees C until imaging.

IF staining for cellular death was performed using the EMD Millipore ApopTag Fluorescein In Situ Apoptosis Detection Kit (S7110), an indirect TUNEL method (34, 35). Terminal deoxynucleotidyl transferase (TdT) modifies genomic DNA for detection of positive cells, and

an anti-digoxigenin antibody is conjugated to a fluorescent reporter. Protocol: fix slides in 1% PFA in 1xPBS (938ul of 16% PFA + 15mL PBS), 2x 5 min rinses in 1xPBS, post fix in pre-cooled 2:1 mix of EtOH:Acetic acid at -20 degrees C, 2x 5 min rinses in 1xPBS, gently dry excess liquid, apply 75ul of Equilibration Buffer per slide for 10 sec, remove excess liquid, apply 55ul of Working Strength TdT Enzyme per slide (77ul Reaction Buffer + 33ul TdT Enzyme), coverslip and place in humidified chamber for 1 hour at 37 degrees C, 10 min in Working Strength Stop/Wash Buffer (1mL stop/wash + 34mL dd$H_2O$), 3x 1 min washes in 1xPBS, apply 65ul Anti-Digoxigenin Conjugate per slide (62ul anti-Digo + 68ul Blocking Solution), coverslip and place in humidified chamber for 30 min at room temperature (keep in dark), 4x 2 min washes in 1xPBS, 2-3 drops of Vectashield Mounting Medium with DAPI (4',6-diamidino-2-phenylindole) per slide, coverslip and dry for several hours in the dark at room temperature, store at -20 degrees C. DAPI fluoresces when bound to DNA and is used as a nuclear counterstain.

All IF slides were imaged using a Leica Microsystems DMI4000 B automated inverted fluorescence microscope with a Hamamatsu ORCA-ER high-resolution digital camera, and using Image-Pro Plus 7.0 software. The Hamamatsu is a black and white camera so all images where taken three times, using blue, green, and red fluorescence. Afterwards, the separate color channels were merged into one, using FIJI/ImageJ software (NIH) (36).

**RNA-sequencing.** Additional samples were cryosectioned for the specific purpose of collecting tissue for RNA-Sequencing. N=3 specimens were collected for each stage (16, 18, and 20 day) and immediately snap-frozen, without fixation, then cryosectioned on Arcturus PEN membrane glass slides (Applied Biosystems), five slides per specimen. An Arcturus Veritas Microdissection Instrument was used for laser capture microdissection (LCM) of Meckel's cartilage and malleus (with minimal surrounding perichondrium) focusing on their connection area. An UV cutting laser was used to excise the tissue of interest. Afterward, an IR capture laser was fired through Arcturus Capsure HS LCM Caps, melting an attached transfer film, which would then bond with

the tissue. The cells attached to the caps were removed with an Arcturus PicoPure RNA Isolation Kit. An ExtracSure Extraction Device was placed on each cap and 10ul of Extraction Buffer (XB) was added to each. A 0.5mL microcentrifuge tube was placed on top, then covered with an incubation block preheated to 42 degrees C, and left to incubate for 30 min. Afterward, they were centrifuged for 2 min at 800x g, the extracted RNA was pooled with the other slides for each specimen, and the cell extract was stored at -80 degrees C. We also took slide scrapes for each set (used for baseline comparison) by placing RNA extraction buffer directly on the slides.

The remainder of the RNA isolation was completed following the PicoPure RNA Isolation Kit guidelines. RNA integrity was checked by an Agilent 2100 Bioanalyzer, revealing RIN values of 7.8 – 8.9. As the quantity of RNA in cartilage is commonly very low, we used the Clontech SMARTer Ultra Low Input RNA Kit for amplification. We began the Clontech amplification with 9ul of pooled RNA from each specimen. The first portion of this protocol, first-strand cDNA synthesis, was completed inside of a PCR clean hood workstation. The final portion, cDNA purification, was completed using Agencourt Ampure XP beads with a magnetic block for separation. All steps were conducted following standard Clontech Kit guidelines, with the final supernatant containing purified cDNA from the original tissue samples stored at -20 degrees C.

Resultant cDNA samples were run through the Bioanalyzer again, as well as a Qubit Fluorometer, to determine accurate concentrations. Next, we built libraries for sequencing using a Nextera XT DNA Sample Preparation Kit, along with a Nextera XT Index Kit and TruSeq Dual Index Sequencing Primers. All samples started with 5ul of input DNA at a concentration of 0.2ng/ul. The standard protocol was followed for the Nextera XT DNA Library Preparation Guide. DNA was tagged and fragmented, amplified via PCR, and cleaned up with AMPure XP beads to purify the library. Afterwards, the library was again validated on the Agilent 2100 Bioanalyzer, followed by library normalization and pooling for HiSeq sequencing. High-

throughput sequencing was conducted on an Illumina HiSeq 2500, at the W.M. Keck Center for Comparative and Functional Genomics at the University of Illinois (37).

Initial RNA-Seq analysis was conducted on the UIUC web-based Galaxy (38) platform (galaxy.illinois.edu), using the Tuxedo protocol. Sequence files were uploaded, along with an opossum reference genome (monDom5) (39) from ensemble.org. The basic sequence for analyses was as follows: Edit Sequences was used to trim ends, TopHat was used to align reads to the genome, Cufflinks was used to assemble the reads into transcripts, Cuffmerge was used to blend multiple samples from the same stage, and Cuffdiff was used to report genes and transcripts that are differentially expressed between samples (40). We also used the Database for Annotation, Visualization and Integrative Discovery (DAVID) Bioinformatics Resource (david.ncifcrf.gov) (41) to identify Gene Ontology (GO) terms describing gene functions for our list of differentially expressed genes and their functionally related gene groups.

**In situ hybridization** - Select genes identified from RNA-Seq were confirmed via fluorescence *in situ* hybrization (FISH) (42), using cryosectioned slides from 16, 18, and 20 day specimens. FISH probes for *TGFbr2* and *WISP1* were designed and manufactured by Molecular Instruments. Each set of probes consists of 5x 20pmole probes with 2x fluorophore labeled hairpins (Alexa488). Protocol was as follows: Day 1- thaw slides, draw hydrophobic circle around tissues with a PAP pen, rinse with DEPC water, 0.2M acid hydrolysis for 15 min (833ul 12M HCL in 50mL DEPC water), wash 2x 5 min in DEPC PBS, wash 1x 6 min in 1ug/mL Proteinase K (1ul in 10mL DEPC PBS), wash 1x 10 min in DPEC PBS, fix with 4% DEPC PFA for 5 min, wash 2x 5 min in DEPC PBS, acetylation with 0.25% acetic acid for 10 min (25ul glacial acetic acid in 10mL DEPC water), wash 2x 5 min in DEPC PBS, pre-hybridize in probe hybridization buffer for 15 min at 45 degrees C, prepare the probe solution (thaw 5 probes on ice, mix 1ul of each probe in 500ul of probe hybridization buffer, warm mixture to 45°C), remove pre-hybridization solution and add probe solution (~150-200ul per slide), cover slip with

parafilm, incubate in humidified chamber overnight (>12 hours) at 45 degrees C. Day 2- remove excess probe with wash buffer (perform washes at 45 degrees C), ~300-500ul of wash buffer per slide, 2x 5 min washes, 2x 30 min washes, 1x 5 min wash, pre-amplify samples in 500ul of amplification buffer for 30 min at room temperature, "snap cool" 2x hairpins (10ul each hairpin in individual PCR tubes, 95 degrees C for 90 seconds in thermal cycler, cool to room temperature in dark drawer for 30 min), mix both hairpins together with 500ul of amplification buffer, remove pre-amplification solution and add hairpin solution (~150-200ul per slide), cover slip with parafilm, incubate in dark overnight (>12 hours) at room temperature. Day 3- remove excess hairpins with 5x SSCT (5x SSC with Tween, 10ul Tween per 10mL of 5x SSC) washes at room temperature, 2x 5 min washes, 2x 30 min washes, 1x 5 min wash, 2-3 drops of Vectashield Mounting Medium with DAPI per slide, glass coverslip, store at 4 degrees C until imaging.

**Functional Assays** - After identifying *TGFbr2* as having a potential role in Meckel's cartilage separation, we knocked down *TGFb* signaling to investigate the impact on phenotype. A TGFb1,2,3 antibody (MAB1835) from R&D Systems was used to neutralize the biological activity of *TGFb* signaling (43). The antibody was reconstituted at 0.5mg/mL in sterile PBS, and 38ul intraperitoneal (IP) injections (based upon estimated 1.9g weight of pups at 20 days) were administered to neonatal opossum for six consecutive days beginning on postnatal day 16. Control pups were injected with an equal dosage of 1xPBS. Mothers were anesthetized with isoflurane during injections. This precluded the necessity of physically removing the pups from the mothers, as the pups are continually attached to the mother's nipples at this developmental stage. We utilized a precision vaporizer isoflurane anesthesia machine with the oxygen flowmeter set to 1 litter per minute (LPM) and the vaporizer dial set to 2½. Mothers were placed in an induction chamber until they lost consciousness, at which point they were switched to a nose cone for the remaining duration. Injections took less than five minutes and the mothers fully recovered within a few minutes after returning to their cages. Pups were euthanized on postnatal day 22. MC morphology was visualized using micro-CT scanning (as described above) and

clearing and staining for at least 3 control and 3 treatment pups. For clearing and staining, following 4% PFA fixation and dehydration into ethanol, P22 samples were placed in acetone, then stained with 0.3% Alcian Blue 8GX (A5268 Sigma) and 0.1% Alizarin Red S (A5533) at 37° C for 5 days. Samples were then cleared in a 1% KOH solution (changed daily) for ~2 weeks. Once cleared, specimens were imaged using a Leica M205 C stereo microscope with a Leica DFC425 digital camera, utilizing the Leica Application Suite (LAS) version 3.8. At least 3 treatment and 3 control pups were also sectioned and IF used to test for apoptotic cells (as described above) and anti-p-Smad2 (44) (at a working concentration of 1:100; otherwise as described above for the Phosphohistone H3 antibody) (Cell Signaling Technology).

**Supplementary Figures:**

**Fig S1.** A - Micro-CT scan image of postnatal day (P) 20 opossum skull with elements relating to the middle ear colored (MC = light green, ectotympanic = purple, goniale = dark green, malleus = light blue, incus = dark blue, and stapes = red). At P20, Meckel's cartilage (MC, light green) rests within the gonial trough (dark green) and is just beginning to detach from the malleus (light blue). B & C – Isolated middle ear structures at P20 in lateral (B) and dorsal (C) view. D – K - Micro-CT scan images of developing opossum skulls at five day increments, beginning on the day of birth through P35, with the middle ear elements colored as in (A). Black arrows indicate separation of MC from the malleus, which first occurs at P20.

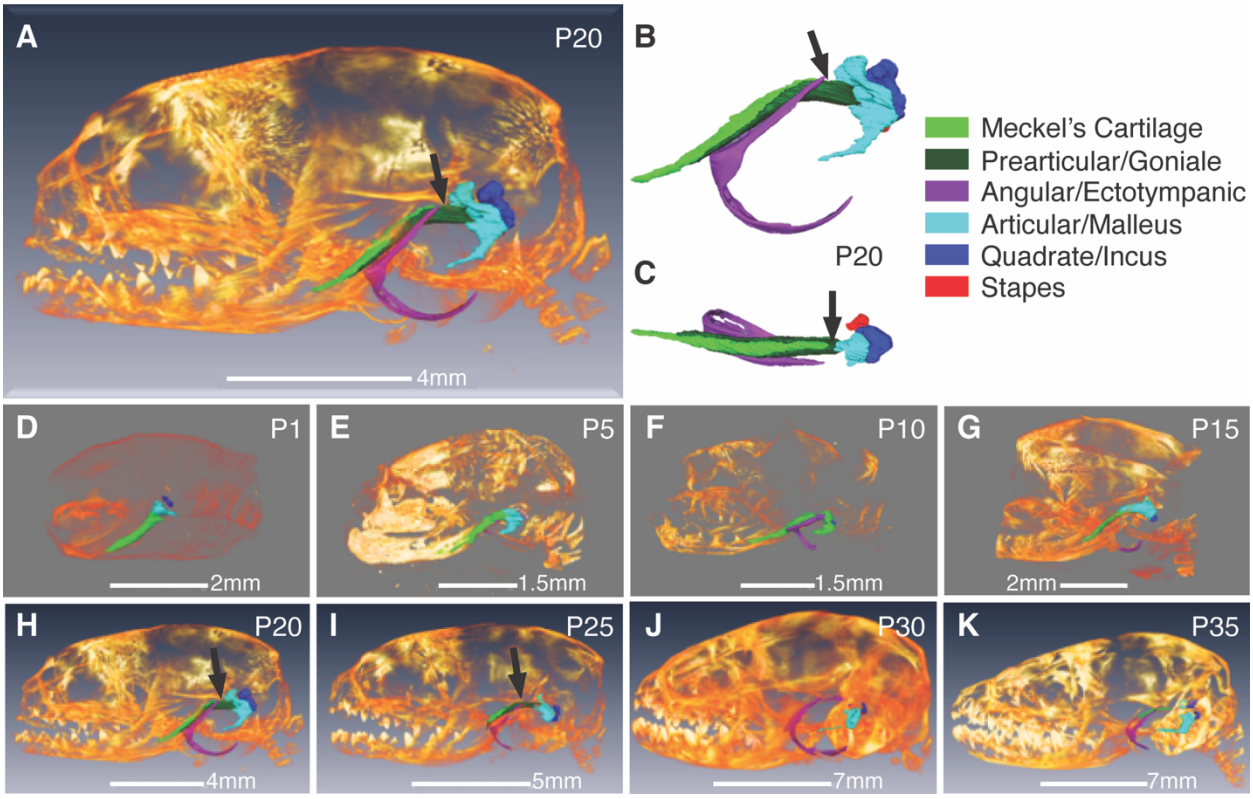

**Fig S2.** Laser tissue capture microdissection was used to extract tissues for RNA-seq. Shown are a representative section before (A) and immediately after (B) laser tissue capture microdissection, and the resultant tissue section that was used for RNA-seq (C).

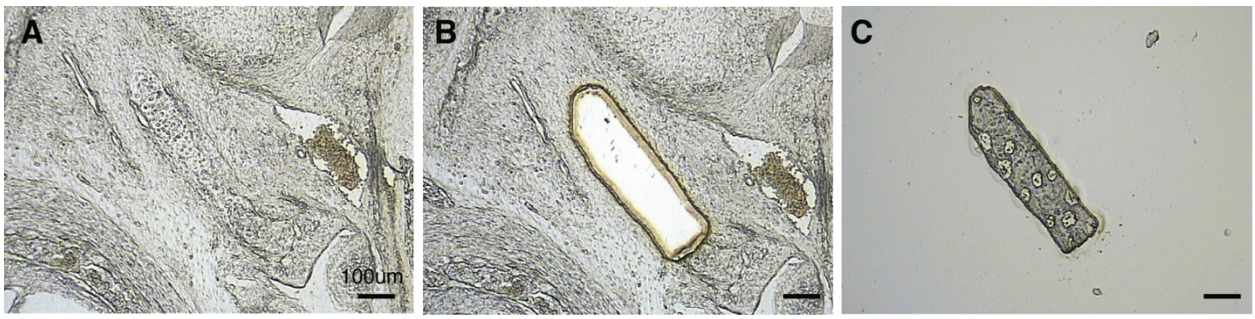

**Fig S3**. Cryosectioned and IF stained slides of the middle ear region. A-D - pSMAD IF stained (green) slides of the comparable ear regions of *TGF-β* neutralizing-antibody treated (A, B, different sections showing the same assay) and control (C, D, different sections showing the same assay) opossums at postnatal day (P) 22, counterstained with the nuclear stain DAPI (blue). pSMAD staining, in this case, is used as a read-out for TGFB signaling. All scale bars = 100um. pSMAD staining is qualitatively more abundant in control (C, D) than *TGF-β* neutralizing-antibody treated (A, B) specimens. (E) The number of pSMAD positive cells was also counted for 11 control and 11 *TGF-β* neutralizing-antibody treated images (taken at the same magnification). Results indicate that there are significantly more pSMAD positive cells in control than *TGF-β* neutralizing-antibody treated images ($P < 0.0001$*). F-G – Positive controls for IF for proliferation (F) and autophagy (G) in opossum middle ear tissues. Representative positive cells are indicated with white arrows. Alt sxn = alternative section.

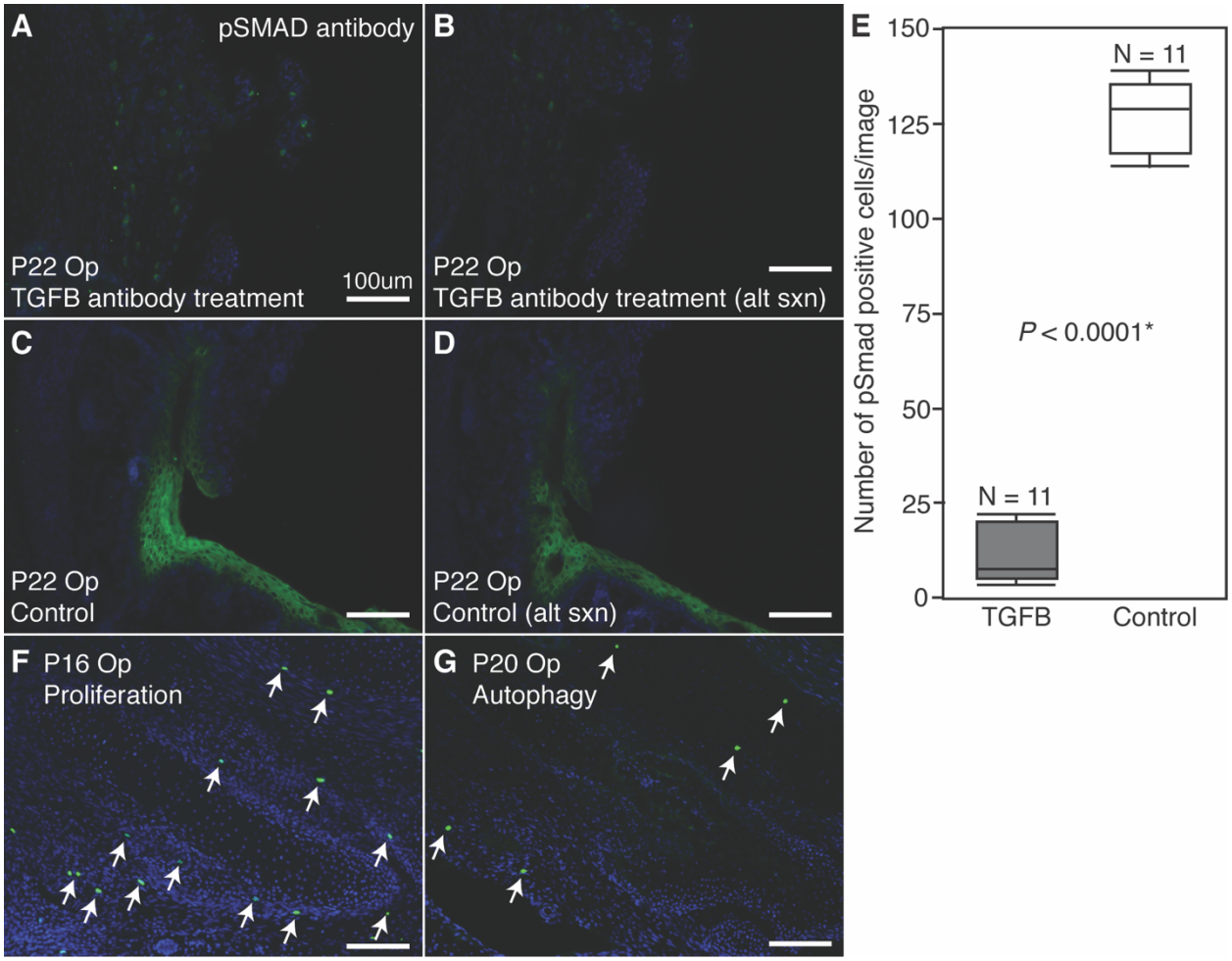
A
pSMAD antibody
P22 Op
TGFB antibody treatment
100um
B
P22 Op
TGFB antibody treatment (alt sxn)
C
P22 Op
Control
D
P22 Op
Control (alt sxn)
E
Number of pSmad positive cells/image
150
125
100
75
50
25
0
N = 11
N = 11
P < 0.0001*
TGFB
Control
F
P16 Op
Proliferation
G
P20 Op
Autophagy

**Fig. S4.** Micro-CT reconstructions in side profile (A-B) and dorsally in conjunction with 2D orthoslice without (C-D) and with (E-F) middle ear elements highlighted in P22 opossum pups. Cleared and stained middle ear structures in side profile (G-H) and dorsal view (I-J). TNA treated pups are shown in A, C, E, G, and I, and control pups in B, D, F, H, and J. A-B – Micro-CT reconstructions with ossified structures of skull more defined (i.e. less opaque) show no pleiotropic deformations caused by TNA treatment. C-F – Dorsal views with 2D slice illustrates how the goniale cradles the MC, and is clearly differentiated from the MC as the goniale is ossified at this point. G-J – Cleared and stained samples show that the posterior end of MC (indicated by black arrows) is detached and partially degraded in control but not TNA specimens. Additionally, the images show no apparent disruption of goniale phenotype.

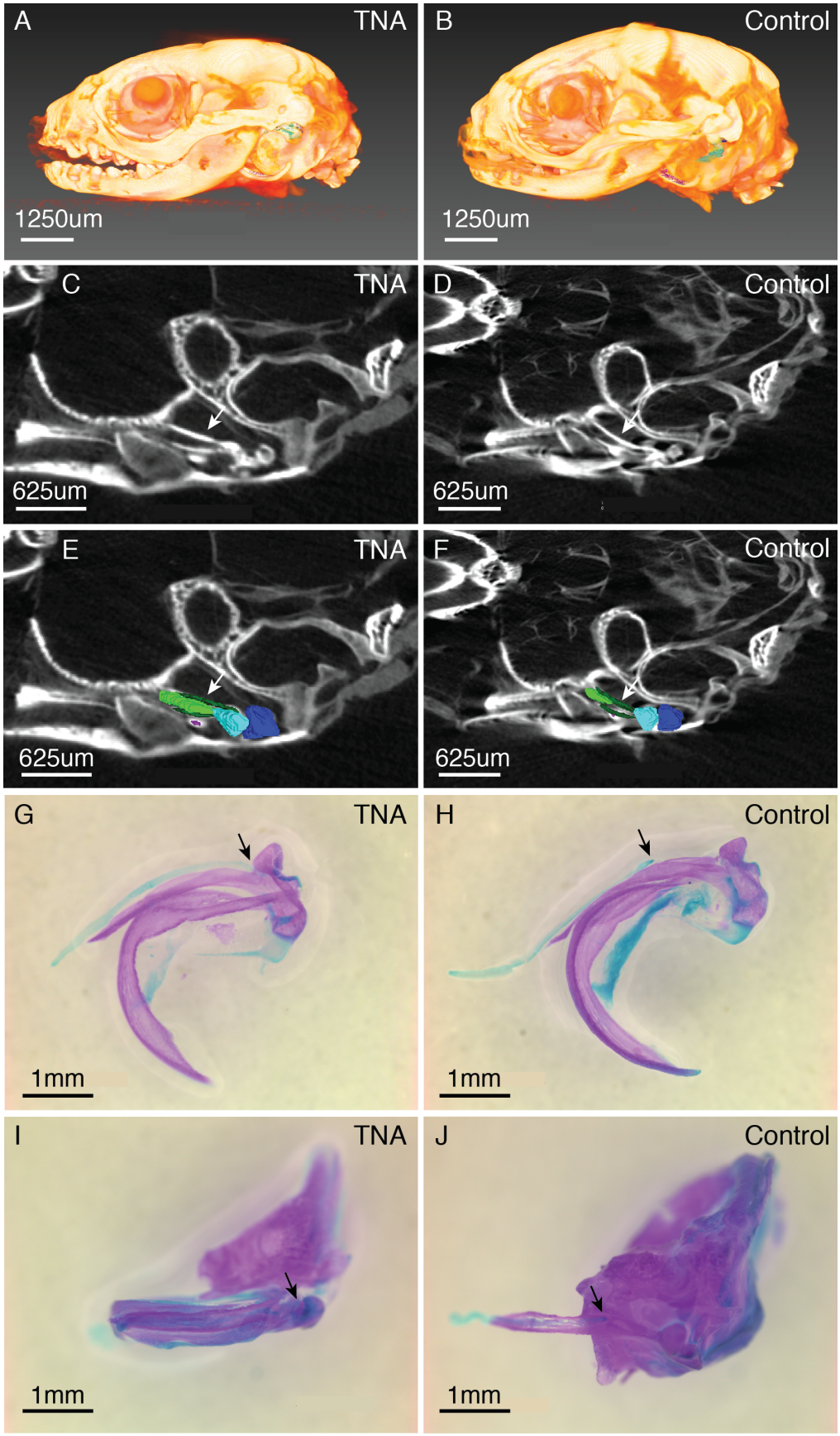
A
TNA
1250um
B
Control
1250um
C
TNA
625um
D
Control
625um
E
TNA
625um
F
Control
625um
G
TNA
1mm
H
Control
1mm
I
TNA
1mm
J
Control
1mm

**Fig S5.** Alternative hypothesis of homoplastic evolution of Mammalian Middle Ears under *TGF-β* signaling. Although the Meckel's sulcus is present in all zatherian stem taxa to crown therians, and in some stem eutherians and metatherians, the ossified Meckel's cartilage itself has not been preserved in these fossils. If treating this as an absence of data, or as presence/absence indeterminate (= "?"), then it is feasible to hypothesize that the theriiform clade (multituberculates + crown therians) had possessed the DMME condition with MC breakdown ancestrally, as documented in multiple multituberculates. If so, an additional evo-devo scenario would also be possible - the presence of ossified Meckel's cartilage in *Maotherium* could be a hypothetical reversal on evolutionary tree, mechanistically possible by a down regulation of gene(s) involved in *TGF-β* signaling (such as *TGF-βR2)* as in the antibody treatment of *TGF-βR2.* It could not be excluded that separate gains of MC breakdown (in monotremes and in theriiforms), and its reversal (only in Maotherium) all occurred in the early history of mammals, given the homoplastic nature of *TGF-β* signaling and its multiple down-cascade developmental processes. Another scenario would be that the Meckel's cartilage was lost in the last common ancestor of marsupials and placentals (the Theria node), following the interpretation that *Peramus* and other stem zatherians retained a MC in the Meckel's sulcus (*53-58*). However, because the Meckel's sulci in stem zatherians are identical to those of basal eutherians (*53-55*) and the metatherian *Kokopelia* (*56*), it is not parsimonious to interpret them differently. Thus we consider the latter scenario to be less likely. All evo-devo hypotheses (Fig. 3 vs. Fig. S5) are contingent on the interpretation of the presence/absence of the MC and its osteological correlates on the dentary in stem eutherians and metatherians, and their immediate zatherian outgroups. But current evidence is more favorable for the scenario presented in Fig 3 than in Fig S5. Our preferred hypothesis is that parallel up regulations of *TGF-β* signaling occurred in multiple early mammal lineages, facilitating the independent acquisitions (Fig 3). However, if the scenario in Fig S5 is correct, then this would suggest that significant developmental systems drift has occurred in modern marsupial and placental mammals. (drawings of *Kokopelia* and *Peramus* courtesy of R. L. Cifelli and B. M. Davis.)

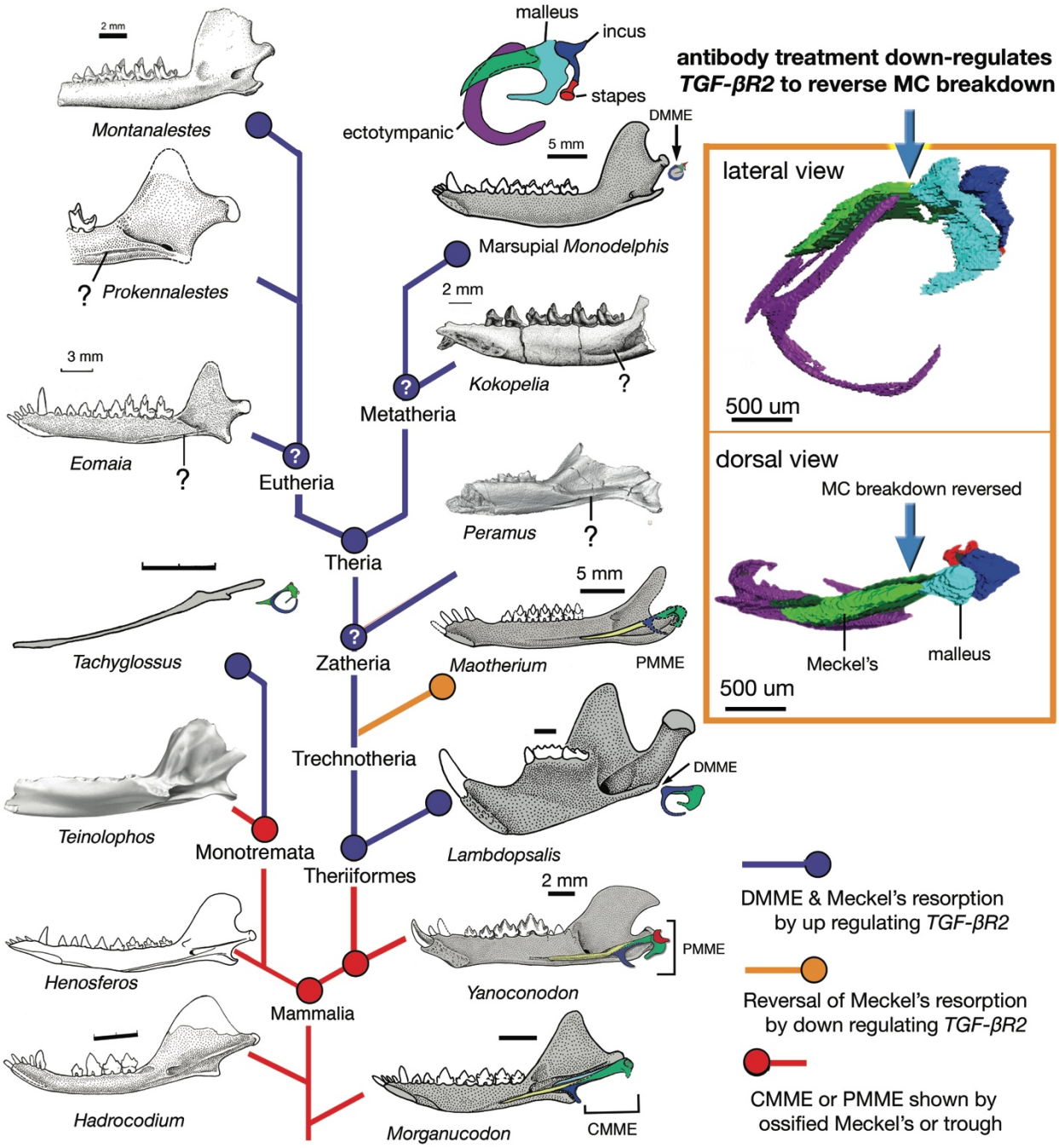
antibody treatment down-regulates
TGF-βR2 to reverse MC breakdown
lateral view
500 um
dorsal view
MC breakdown reversed
Meckel's
malleus
500 um
malleus
incus
stapes
ectotympanic
DMME
5 mm
Marsupial Monodelphis
2 mm
Kokopelia
?
Metatheria
Montanalestes
2 mm
? Prokennalestes
3 mm
Eomaia
?
Eutheria
Peramus
?
Theria
5 mm
Tachyglossus
Zatheria
Maotherium
PMME
Trechnotheria
DMME
Teinolophos
Lambdopsalis
Monotremata
Theriiformes
2 mm
Henosferos
PMME
Yanoconodon
Mammalia
Hadrocodium
Morganucodon
CMME
DMME & Meckel's resorption
by up regulating TGF-βR2
Reversal of Meckel's resorption
by down regulating TGF-βR2
CMME or PMME shown by
ossified Meckel's or trough

**Tables:**

Table S1. Genes that are differentially expressed in the opossum Meckel's cartilage and its perichondrium by a log-fold change of ≥2 at and before P20 (Sample1 = P16 or P18, and Sample2 = P20), as identified by RNA-seq.

| Gene Name | Sample1 | Value1 | Sample2 | Value2 | log2(fold_change) | P_value |
|---|---|---|---|---|---|---|
| *CRYGN* | P16 | 0.8324 | P20 | 75.8965 | 6.5107 | 0.0003 |
| *SLC30A1* | P16 | 0.3747 | P20 | 20.4888 | 5.7728 | 0.0001 |
| *CRYGN* | P18 | 1.6332 | P20 | 75.8965 | 5.5383 | 0.0002 |
| *MOB3A* | P16 | 0.2553 | P20 | 9.2157 | 5.1739 | 0.0003 |
| *GPNMB* | P16 | 5.4177 | P20 | 193.4330 | 5.1580 | 0.0001 |
| *F10* | P16 | 0.3024 | P20 | 9.6712 | 4.9991 | 0.0002 |
| *HEYL* | P16 | 0.2930 | P20 | 7.5006 | 4.6780 | 0.0003 |
| *CLIC2* | P16 | 0.3666 | P20 | 8.8372 | 4.5913 | 0.0005 |
| *SLC13A5* | P16 | 0.9642 | P20 | 23.2089 | 4.5892 | 0.0001 |
| *LAT* | P16 | 1.6472 | P20 | 39.5272 | 4.5848 | 0.0004 |
| *PHLDA3* | P16 | 3.1026 | P20 | 71.7884 | 4.5322 | 0.0001 |
| *MRGPRF* | P16 | 0.3743 | P20 | 8.5915 | 4.5205 | 0.0004 |
| *ABCB8* | P16 | 1.2166 | P20 | 26.8737 | 4.4652 | 0.0001 |
| *ABCD4* | P16 | 0.2849 | P20 | 6.2188 | 4.4483 | 0.0006 |
| *TOR1B* | P16 | 0.3877 | P20 | 8.2769 | 4.4159 | 0.0004 |
| *ANAPC2* | P16 | 0.4689 | P20 | 9.8237 | 4.3890 | 0.0001 |
| *CHN2* | P16 | 0.6339 | P20 | 13.2001 | 4.3801 | 0.0001 |
| *PEX19* | P16 | 1.5901 | P20 | 33.0957 | 4.3794 | 0.0004 |
| *CAP1* | P16 | 4.6801 | P20 | 97.1644 | 4.3758 | 0.0003 |
| *SESN1* | P16 | 0.9021 | P20 | 17.6288 | 4.2884 | 0.0001 |

| | | | | | | |
|---|---|---|---|---|---|---|
| *RND3* | P16 | 0.9627 | P20 | 18.3046 | 4.2490 | 0.0003 |
| *PEX5* | P16 | 0.4076 | P20 | 7.3453 | 4.1714 | 0.0001 |
| *IRAK2* | P16 | 0.5860 | P20 | 10.3899 | 4.1483 | 0.0001 |
| *FGF1* | P16 | 0.9807 | P20 | 17.3449 | 4.1445 | 0.0002 |
| *IL13RA1* | P16 | 0.5382 | P20 | 9.3901 | 4.1249 | 0.0002 |
| *COL10A1* | P16 | 2.3641 | P20 | 40.9610 | 4.1149 | 0.0004 |
| *NHLRC3* | P16 | 0.9749 | P20 | 16.8160 | 4.1084 | 0.0003 |
| *RELL1* | P16 | 0.7694 | P20 | 13.1456 | 4.0948 | 0.0003 |
| *PLA1A* | P16 | 0.2976 | P20 | 5.0599 | 4.0878 | 0.0006 |
| *CA7* | P16 | 4.5772 | P20 | 76.6977 | 4.0667 | 0.0001 |
| *LYRM2* | P16 | 2.6861 | P20 | 44.9668 | 4.0653 | 0.0004 |
| *LDHB* | P16 | 7.4146 | P20 | 123.9810 | 4.0636 | 0.0005 |
| *CYB5R1* | P16 | 2.4520 | P20 | 40.7501 | 4.0548 | 0.0004 |
| *ATP6V1H* | P16 | 1.9625 | P20 | 32.1239 | 4.0329 | 0.0002 |
| *CYP1B1* | P16 | 2.3490 | P20 | 38.1663 | 4.0222 | 0.0001 |
| *PTPRJ* | P16 | 0.7220 | P20 | 11.0466 | 3.9355 | 0.0002 |
| *CAPN1* | P16 | 0.6118 | P20 | 9.3096 | 3.9275 | 0.0002 |
| *TBC1D8B* | P16 | 0.2400 | P20 | 3.6126 | 3.9122 | 0.0005 |
| *WFDC1* | P16 | 5.9516 | P20 | 88.6521 | 3.8968 | 0.0002 |
| *TMEM176A* | P16 | 2.3058 | P20 | 33.8702 | 3.8767 | 0.0004 |
| *SMPD1* | P16 | 7.9985 | P20 | 116.4700 | 3.8641 | 0.0006 |
| *FBXL5* | P16 | 0.7049 | P20 | 10.2397 | 3.8605 | 0.0002 |
| *SRPX2* | P16 | 1.9418 | P20 | 27.3680 | 3.8170 | 0.0001 |
| *RNF149* | P16 | 1.5006 | P20 | 21.0959 | 3.8133 | 0.0003 |
| *UBALD1* | P18 | 0.2886 | P20 | 3.9707 | 3.7823 | 0.0006 |

| | | | | | | |
|---|---|---|---|---|---|---|
| *SH3GLB1* | P16 | 4.5504 | P20 | 61.9177 | 3.7663 | 0.0004 |
| *PSTPIP1* | P16 | 3.8211 | P20 | 51.7928 | 3.7607 | 0.0005 |
| *TEX264* | P16 | 2.5089 | P20 | 33.9832 | 3.7597 | 0.0006 |
| *ATP6V1G1* | P16 | 14.2728 | P20 | 191.9410 | 3.7493 | 0.0001 |
| *LDHA* | P16 | 4.8011 | P20 | 62.3381 | 3.6987 | 0.0001 |
| *NPEPL1* | P16 | 1.7956 | P20 | 23.2428 | 3.6943 | 0.0002 |
| *GUSB* | P16 | 18.2832 | P20 | 236.2410 | 3.6917 | 0.0002 |
| *TGFBR2* | P16 | 1.7625 | P20 | 22.7159 | 3.6880 | 0.0001 |
| *CSTB* | P16 | 28.9600 | P20 | 356.9720 | 3.6237 | 0.0001 |
| *NELFE* | P16 | 4.4724 | P20 | 55.0475 | 3.6216 | 0.0004 |
| *SLC15A4* | P16 | 7.0713 | P20 | 86.0409 | 3.6050 | 0.0002 |
| *GNPTAB* | P16 | 6.8039 | P20 | 82.6563 | 3.6027 | 0.0001 |
| *ATP6V1A* | P16 | 7.1738 | P20 | 86.1035 | 3.5853 | 0.0001 |
| *RPS6KB2* | P16 | 11.1784 | P20 | 132.9680 | 3.5723 | 0.0004 |
| *PSMD11* | P16 | 3.6688 | P20 | 43.4043 | 3.5645 | 0.0001 |
| *EMC3* | P16 | 3.0389 | P20 | 35.8801 | 3.5616 | 0.0004 |
| *AAGAB* | P16 | 1.6075 | P20 | 18.6800 | 3.5386 | 0.0003 |
| *EIF2A* | P16 | 1.4181 | P20 | 16.4793 | 3.5386 | 0.0005 |
| *ACAD9* | P16 | 1.5728 | P20 | 18.0065 | 3.5171 | 0.0006 |
| *ADAM15* | P16 | 2.1646 | P20 | 24.4993 | 3.5006 | 0.0001 |
| *PFKL* | P16 | 3.1802 | P20 | 35.5393 | 3.4822 | 0.0001 |
| *ANKH* | P16 | 5.9964 | P20 | 66.6633 | 3.4747 | 0.0004 |
| *LCP1* | P16 | 3.2972 | P20 | 36.1764 | 3.4557 | 0.0001 |
| *CERCAM* | P16 | 5.1337 | P20 | 55.4056 | 3.4320 | 0.0001 |
| *ALPL* | P16 | 27.7116 | P20 | 296.4290 | 3.4191 | 0.0001 |

| | | | | | | |
|---|---|---|---|---|---|---|
| *SPP1* | P16 | 338.7830 | P20 | 3610.3400 | 3.4137 | 0.0004 |
| *NDUFS1* | P16 | 2.1621 | P20 | 22.8393 | 3.4010 | 0.0001 |
| *FOS* | P16 | 2.5663 | P20 | 27.0343 | 3.3970 | 0.0001 |
| *FBXW5* | P16 | 3.0730 | P20 | 32.3598 | 3.3965 | 0.0001 |
| *ZNF212* | P18 | 0.9259 | P20 | 9.7384 | 3.3947 | 0.0003 |
| *ISCA1* | P16 | 1.8158 | P20 | 19.0385 | 3.3903 | 0.0002 |
| *PHC2* | P16 | 1.9818 | P20 | 20.6799 | 3.3833 | 0.0001 |
| *DOHH* | P16 | 4.1690 | P20 | 43.3923 | 3.3797 | 0.0001 |
| *CDKN1A* | P16 | 2.6423 | P20 | 27.4103 | 3.3749 | 0.0002 |
| *PAMR1* | P16 | 4.8940 | P20 | 50.7366 | 3.3740 | 0.0006 |
| *ALDH1L2* | P16 | 2.1907 | P20 | 22.7000 | 3.3732 | 0.0001 |
| *LGMN* | P16 | 5.0190 | P20 | 51.9234 | 3.3709 | 0.0006 |
| *EXOSC10* | P16 | 1.3799 | P20 | 14.1384 | 3.3570 | 0.0002 |
| *THOC3* | P16 | 1.7299 | P20 | 17.6879 | 3.3540 | 0.0001 |
| *RAB38* | P16 | 5.5933 | P20 | 56.3397 | 3.3324 | 0.0001 |
| *TTLL9* | P18 | 4.0606 | P20 | 40.8482 | 3.3305 | 0.0001 |
| *NQO1* | P16 | 7.9475 | P20 | 79.9176 | 3.3299 | 0.0001 |
| *TGFBI* | P16 | 8.1163 | P20 | 81.6119 | 3.3299 | 0.0001 |
| *CD200* | P16 | 7.7808 | P20 | 78.2029 | 3.3292 | 0.0003 |
| *C1orf198* | P16 | 1.3587 | P20 | 13.6550 | 3.3292 | 0.0001 |
| *ZNF212* | P16 | 0.9826 | P20 | 9.7384 | 3.3090 | 0.0003 |
| *C16orf72* | P16 | 2.4425 | P20 | 24.1595 | 3.3062 | 0.0001 |
| *AGFG1* | P16 | 0.8293 | P20 | 8.1228 | 3.2920 | 0.0002 |
| *CCNG1* | P16 | 5.6563 | P20 | 55.0936 | 3.2840 | 0.0001 |
| *BLVRB* | P16 | 6.3890 | P20 | 62.2087 | 3.2835 | 0.0004 |

| | | | | | | |
|---|---|---|---|---|---|---|
| *SMIM14* | P16 | 2.4568 | P20 | 23.8276 | 3.2778 | 0.0004 |
| *SEC23IP* | P16 | 0.8076 | P20 | 7.8010 | 3.2720 | 0.0001 |
| *EI24* | P16 | 6.7958 | P20 | 65.5888 | 3.2707 | 0.0001 |
| *SRM* | P16 | 8.8766 | P20 | 85.5215 | 3.2682 | 0.0001 |
| *CMAS* | P16 | 3.8087 | P20 | 36.4443 | 3.2583 | 0.0001 |
| *MAMDC2* | P16 | 1.1091 | P20 | 10.5743 | 3.2531 | 0.0001 |
| *DUSP7* | P16 | 2.0387 | P20 | 19.3555 | 3.2470 | 0.0002 |
| *IL21R* | P18 | 1.2314 | P20 | 11.6860 | 3.2464 | 0.0004 |
| *HERPUD1* | P16 | 4.2197 | P20 | 39.8036 | 3.2377 | 0.0001 |
| *MME* | P16 | 9.7353 | P20 | 91.7013 | 3.2356 | 0.0003 |
| *TMEM127* | P16 | 4.2297 | P20 | 39.7176 | 3.2312 | 0.0004 |
| *ELP6* | P16 | 1.9598 | P20 | 18.3946 | 3.2305 | 0.0003 |
| *NDFIP1* | P16 | 11.4032 | P20 | 105.0680 | 3.2038 | 0.0002 |
| *BGLAP* | P16 | 339.9940 | P20 | 3088.9700 | 3.1835 | 0.0001 |
| *UBE2O* | P16 | 1.1107 | P20 | 9.9429 | 3.1622 | 0.0004 |
| *LEMD2* | P16 | 1.7026 | P20 | 15.1901 | 3.1573 | 0.0003 |
| *EEF2* | P16 | 2.9179 | P20 | 25.7080 | 3.1392 | 0.0006 |
| *COPG1* | P16 | 4.5783 | P20 | 40.0315 | 3.1282 | 0.0002 |
| *RAP1B* | P16 | 5.2698 | P20 | 45.8499 | 3.1211 | 0.0004 |
| *ATP6V0E1* | P16 | 16.7800 | P20 | 144.0400 | 3.1017 | 0.0002 |
| *ATP5A1* | P16 | 13.9893 | P20 | 119.9680 | 3.1003 | 0.0001 |
| *STAT3* | P16 | 3.1351 | P20 | 26.8130 | 3.0964 | 0.0001 |
| *COPS4* | P16 | 3.5697 | P20 | 30.4541 | 3.0928 | 0.0005 |
| *ACAA1* | P16 | 25.4232 | P20 | 216.4430 | 3.0898 | 0.0002 |
| *SHROOM4* | P16 | 0.7053 | P20 | 5.9220 | 3.0698 | 0.0001 |

| | | | | | | |
|---|---|---|---|---|---|---|
| *RPN2* | P16 | 12.5821 | P20 | 105.5130 | 3.0680 | 0.0003 |
| *TWISTNB* | P16 | 5.0284 | P20 | 42.1052 | 3.0658 | 0.0002 |
| *EDEM2* | P16 | 3.0920 | P20 | 25.8693 | 3.0646 | 0.0002 |
| *LSM6* | P16 | 1.6086 | P20 | 13.4273 | 3.0613 | 0.0004 |
| *RPS27L* | P16 | 4.7378 | P20 | 39.5277 | 3.0606 | 0.0003 |
| *ADAM15* | P18 | 2.9377 | P20 | 24.4993 | 3.0600 | 0.0002 |
| *DNAJB11* | P16 | 13.6788 | P20 | 114.0590 | 3.0598 | 0.0002 |
| *CRAT* | P18 | 2.9422 | P20 | 24.5235 | 3.0592 | 0.0005 |
| *U6* | P16 | 1.5852 | P20 | 13.0980 | 3.0466 | 0.0002 |
| *BHLHE40* | P16 | 1.4196 | P20 | 11.6905 | 3.0418 | 0.0002 |
| *MRPS34* | P16 | 3.7075 | P20 | 30.4121 | 3.0361 | 0.0003 |
| *WISP1* | P16 | 8.6652 | P20 | 70.6432 | 3.0273 | 0.0001 |
| *TRIM35* | P16 | 1.1764 | P20 | 9.5519 | 3.0214 | 0.0002 |
| *LGALS3* | P16 | 7.1541 | P20 | 57.7651 | 3.0134 | 0.0001 |
| *RTN4* | P16 | 10.3529 | P20 | 83.5046 | 3.0118 | 0.0004 |
| *DERL1* | P16 | 2.7446 | P20 | 22.1139 | 3.0103 | 0.0001 |
| *NDUFA8* | P16 | 8.9907 | P20 | 72.4168 | 3.0098 | 0.0002 |
| *YIPF3* | P16 | 18.6898 | P20 | 150.4320 | 3.0088 | 0.0002 |
| *PDZD8* | P16 | 1.2030 | P20 | 9.6810 | 3.0086 | 0.0002 |
| *ARL6IP5* | P16 | 18.6137 | P20 | 149.4410 | 3.0051 | 0.0001 |
| *TOR1A* | P16 | 2.4346 | P20 | 19.5142 | 3.0028 | 0.0002 |
| *SLC25A3* | P16 | 19.9596 | P20 | 159.5180 | 2.9986 | 0.0001 |
| *GGT5* | P16 | 9.2224 | P20 | 73.4474 | 2.9935 | 0.0003 |
| *CYBA* | P16 | 43.3230 | P20 | 343.1310 | 2.9856 | 0.0003 |
| *MRPL17* | P16 | 2.2576 | P20 | 17.8413 | 2.9824 | 0.0003 |

| | | | | | | |
|---|---|---|---|---|---|---|
| *IPO9* | P18 | 1.8207 | P20 | 14.3420 | 2.9777 | 0.0002 |
| *CAT* | P16 | 3.2957 | P20 | 25.9307 | 2.9760 | 0.0004 |
| *TIMP2* | P16 | 3.8181 | P20 | 29.8808 | 2.9683 | 0.0003 |
| *COL5A2* | P16 | 59.3856 | P20 | 464.7180 | 2.9682 | 0.0003 |
| *ACTR10* | P16 | 1.2681 | P20 | 9.8580 | 2.9586 | 0.0004 |
| *THOC3* | P18 | 2.2755 | P20 | 17.6879 | 2.9585 | 0.0002 |
| *LTBR* | P16 | 6.3426 | P20 | 49.1095 | 2.9529 | 0.0003 |
| *PRSS23* | P16 | 4.4049 | P20 | 34.0243 | 2.9494 | 0.0001 |
| *AAR2* | P16 | 0.9889 | P20 | 7.6348 | 2.9487 | 0.0004 |
| *CDH15* | P16 | 1.8866 | P20 | 14.5234 | 2.9445 | 0.0003 |
| *MXD4* | P16 | 5.2881 | P20 | 40.1154 | 2.9233 | 0.0002 |
| *PDLIM7* | P16 | 13.1429 | P20 | 99.4072 | 2.9191 | 0.0002 |
| *TIMM50* | P16 | 2.1672 | P20 | 16.3617 | 2.9164 | 0.0003 |
| *SPNS1* | P16 | 4.6489 | P20 | 35.0264 | 2.9135 | 0.0004 |
| *LRPAP1* | P16 | 21.9156 | P20 | 164.5920 | 2.9089 | 0.0001 |
| *GAS1* | P16 | 1.4824 | P20 | 11.0917 | 2.9035 | 0.0003 |
| *PDIA5* | P16 | 3.3190 | P20 | 24.6629 | 2.8935 | 0.0001 |
| *HIF1A* | P16 | 3.8875 | P20 | 28.7906 | 2.8887 | 0.0002 |
| *CORO1B* | P16 | 2.6870 | P20 | 19.8885 | 2.8879 | 0.0005 |
| *HM13* | P16 | 18.4673 | P20 | 136.5720 | 2.8866 | 0.0005 |
| *TMED7TICAM2* | P16 | 3.3149 | P20 | 24.3223 | 2.8753 | 0.0001 |
| *DYNLT3* | P18 | 2.1378 | P20 | 15.6742 | 2.8742 | 0.0003 |
| *LDLRAP1* | q1 | 1.8955 | P20 | 13.7809 | 2.8620 | 0.0002 |
| *MRPL44* | q1 | 1.2940 | P20 | 9.3757 | 2.8571 | 0.0005 |
| *RAP2A* | q1 | 1.0080 | P20 | 7.2773 | 2.8519 | 0.0006 |

| | | | | | | |
|---|---|---|---|---|---|---|
| *EIF4H* | q1 | 5.3779 | P20 | 38.6516 | 2.8454 | 0.0004 |
| *CD44* | q1 | 2.6598 | P20 | 19.0495 | 2.8404 | 0.0001 |
| *SLC38A2* | q1 | 4.1330 | P20 | 29.5496 | 2.8379 | 0.0001 |
| *TP53INP1* | q1 | 1.4336 | P20 | 10.2464 | 2.8374 | 0.0005 |
| *ANXA2* | q1 | 114.7870 | P20 | 815.9270 | 2.8295 | 0.0004 |
| *SLC6A6* | q1 | 4.1070 | P20 | 29.1402 | 2.8268 | 0.0006 |
| *SMURF2* | q1 | 0.6967 | P20 | 4.9223 | 2.8208 | 0.0003 |
| *BTG1* | q1 | 30.3017 | P20 | 213.9780 | 2.8200 | 0.0001 |
| *ACTR1B* | q1 | 2.6992 | P20 | 19.0422 | 2.8186 | 0.0003 |
| *SHROOM4* | q2 | 0.8410 | P20 | 5.9220 | 2.8159 | 0.0003 |
| *SLC30A1* | q2 | 2.9107 | P20 | 20.4888 | 2.8154 | 0.0001 |
| *KCTD17* | P16 | 2.3516 | P20 | 16.3364 | 2.7964 | 0.0003 |
| *PEX12* | P16 | 3.3597 | P20 | 23.3272 | 2.7956 | 0.0004 |
| *TSC22D1* | P16 | 13.0848 | P20 | 90.0301 | 2.7825 | 0.0003 |
| *CNOT10* | P16 | 1.6229 | P20 | 11.1560 | 2.7812 | 0.0004 |
| *KDELR2* | P16 | 7.8427 | P20 | 53.6487 | 2.7741 | 0.0001 |
| *ATP2B1* | P16 | 4.0235 | P20 | 27.1793 | 2.7560 | 0.0006 |
| *SGSM3* | P18 | 4.4041 | P20 | 29.6479 | 2.7510 | 0.0001 |
| *DCAF7* | P16 | 3.6234 | P20 | 24.3811 | 2.7504 | 0.0004 |
| *GANAB* | P16 | 8.0740 | P20 | 54.2670 | 2.7487 | 0.0006 |
| *SERP1* | P16 | 9.7854 | P20 | 65.7051 | 2.7473 | 0.0002 |
| *PRKAB1* | P16 | 1.6513 | P20 | 11.0815 | 2.7465 | 0.0002 |
| *SNAI2* | P16 | 15.4730 | P20 | 103.7610 | 2.7454 | 0.0005 |
| *SNX2* | P16 | 9.9401 | P20 | 66.5531 | 2.7432 | 0.0001 |
| *CAPZA1* | P16 | 10.9147 | P20 | 73.0238 | 2.7421 | 0.0003 |

| | | | | | | |
|---|---|---|---|---|---|---|
| *CYP1B1* | P18 | 5.7072 | P20 | 38.1663 | 2.7415 | 0.0003 |
| *UBE2B* | P16 | 25.7263 | P20 | 171.7000 | 2.7386 | 0.0005 |
| *PCMT1* | P16 | 6.5489 | P20 | 43.6257 | 2.7359 | 0.0001 |
| *GPC1* | P16 | 2.9899 | P20 | 19.7578 | 2.7243 | 0.0005 |
| *ARCN1* | P16 | 5.8986 | P20 | 38.8380 | 2.7190 | 0.0001 |
| *CRYZ* | P16 | 13.2038 | P20 | 86.5681 | 2.7129 | 0.0001 |
| *FKBP14* | P16 | 23.6648 | P20 | 154.7210 | 2.7089 | 0.0001 |
| *RNF149* | P18 | 3.2361 | P20 | 21.0959 | 2.7046 | 0.0003 |
| *CKAP4* | P16 | 17.4912 | P20 | 113.6620 | 2.7001 | 0.0001 |
| *PHGDH* | P16 | 5.1652 | P20 | 33.5483 | 2.6993 | 0.0005 |
| *TFE3* | P16 | 4.6872 | P20 | 30.3308 | 2.6940 | 0.0006 |
| *LAMC1* | P16 | 2.4734 | P20 | 15.9447 | 2.6885 | 0.0003 |
| *ARF4* | P16 | 14.2977 | P20 | 92.0415 | 2.6865 | 0.0002 |
| *KIAA2013* | P16 | 3.1185 | P20 | 19.8441 | 2.6698 | 0.0005 |
| *HPGD* | P16 | 2.7963 | P20 | 17.7919 | 2.6697 | 0.0004 |
| *MAT2A* | P16 | 5.2932 | P20 | 33.6077 | 2.6666 | 0.0006 |
| *GPNMB* | P16 | 5.4177 | P20 | 34.2538 | 2.6605 | 0.0003 |
| *TPBG* | P16 | 4.6269 | P20 | 29.1919 | 2.6575 | 0.0002 |
| *PIGT* | P16 | 22.0115 | P20 | 138.5010 | 2.6536 | 0.0003 |
| *RBM8A* | P16 | 5.6275 | P20 | 35.0975 | 2.6408 | 0.0001 |
| *MDFI* | P16 | 7.6713 | P20 | 47.7377 | 2.6376 | 0.0004 |
| *OSTC* | P16 | 24.7118 | P20 | 151.6430 | 2.6174 | 0.0001 |
| *PNRC1* | P16 | 9.4137 | P20 | 56.8202 | 2.5936 | 0.0002 |
| *PRKCDBP* | P16 | 6.9837 | P20 | 42.0017 | 2.5884 | 0.0002 |
| *JAG1* | P16 | 0.6121 | P20 | 3.5495 | 2.5358 | 0.0004 |

| | | | | | | |
|---|---|---|---|---|---|---|
| *EPRS* | P16 | 6.8668 | P20 | 39.6481 | 2.5295 | 0.0002 |
| *EFCAB14* | P16 | 5.0970 | P20 | 29.4241 | 2.5293 | 0.0005 |
| *GPX7* | P16 | 5.9311 | P20 | 34.2052 | 2.5278 | 0.0002 |
| *EIF3D* | P16 | 15.4771 | P20 | 88.6152 | 2.5174 | 0.0006 |
| *CALU* | P16 | 22.6371 | P20 | 128.6070 | 2.5062 | 0.0006 |
| *LMAN1* | P16 | 6.2334 | P20 | 33.6614 | 2.4330 | 0.0002 |
| *LUM* | P16 | 53.1506 | P20 | 283.6810 | 2.4161 | 0.0003 |
| *CRTAP* | P16 | 10.9128 | P20 | 58.1254 | 2.4132 | 0.0001 |
| *ANXA1* | P16 | 8.9166 | P20 | 47.4461 | 2.4117 | 0.0003 |
| *WDR1* | P16 | 6.6354 | P20 | 34.0139 | 2.3579 | 0.0003 |
| *EIF3E* | P16 | 11.2570 | P20 | 57.5368 | 2.3537 | 0.0003 |
| *DYNC1H1* | P16 | 1.4542 | P20 | 7.2336 | 2.3145 | 0.0005 |
| *SLK* | P16 | 2.6246 | P20 | 12.9263 | 2.3001 | 0.0002 |
| *SFRP2* | P16 | 11.4798 | P20 | 54.9579 | 2.2592 | 0.0006 |
| *COL5A1* | P16 | 7.8880 | P20 | 37.6069 | 2.2533 | 0.0006 |
| *PSMA6* | P16 | 11.2671 | P20 | 53.5942 | 2.2500 | 0.0004 |
| *PSMC4* | P16 | 8.4349 | P20 | 39.4978 | 2.2273 | 0.0003 |
| *RPS27A* | P16 | 270.8450 | P20 | 1219.8700 | 2.1712 | 0.0001 |

**References:**


32. Cooper KL, Sears KE, Uygur A, Maier JA, Baczkowski KS, *et al.* (2014) Patterning and post-patterning modes of evolutionary digit loss in mammals. *Nature* 511(7507):41-45.

33. Dowling A, Doroba C, Maier JA, Cohen L, Vandeberg J, *et al.* (2016) Cellular and molecular drivers of differential organ growth: insights from the limbs of *Monodelphis domestica*. *Dev Genes Evol*:1-9.

34. Molineaux AC, Maier JA, Schecker T, & Sears KE (2015) Exogenous retinoic acid induces digit reduction in opossums (*Monodelphis domestica*) by disrupting cell death and proliferation, and apical ectodermal ridge and zone of polarizing activity function. *Birth Defects Res A Clin Mol Teratol* 103(3):225-234.

35. Hübler M, Niswander L, Peters J, & Sears KE (2010) The developmental reduction of the marsupial coracoid: A case study in *Monodelphis domestica*. *J Morphol* 271(7):769-776.

36. Schindelin J*,* Arganda-Carreras I, Frise E, Kaynig V, Mongair M, *et al.* (2012) Fiji: an open-source platform for biological-image analysis. *Nature Methods* 9(7):676-682.

37. Sears KE*,* Maier JA, Rivas-Astroza M, Poe R, Zhong S, *et al.* (2015) The relationship between gene network structure and expression variation among individuals and species. *PLoS Genet* 11(8):e1005398.

38. Afgan E*,* Baker D, van den Beek M, Blankenberg D, Bouvier D, *et al.* (2016) The Galaxy platform for accessible, reproducible and collaborative biomedical analyses: 2016 update. *Nucleic Acids Res*:gkw343.

39. Mikkelsen TS*,* Wakefield MJ, Aken B, Amemiya CT, Chang JL, *et al.* (2007) Genome of the marsupial *Monodelphis domestica* reveals innovation in non-coding sequences. *Nature* 447(7141):167-177.

40. Trapnell C*,* Roberts A, Goff L, Pertea G, Kim D, *et al.* (2012) Differential gene and transcript expression analysis of RNA-seq experiments with TopHat and Cufflinks. *Nature Protoc* 7(3):562-578.

41. Huang DW, Sherman BT, & Lempicki RA (2009) Systematic and integrative analysis of large gene lists using DAVID bioinformatics resources. *Nature Protoc* 4(1):44-57.

42. Maier JA, Lo YT, & Harfe BD (2013) *Foxa1* and *Foxa2* are required for formation of the intervertebral discs. *PloS one* 8(1):e55528.

43. Dasch JR, Pace DR, Waegell W, Inenaga D, & Ellingsworth L (1989) Monoclonal antibodies recognizing transforming growth factor-beta. Bioactivity neutralization and transforming growth factor beta 2 affinity purification. *J Immunol* 142(5):1536-1541.

44. Anthwal N, Chai Y, & Tucker AS (2008) The role of transforming growth factor-β signalling in the patterning of the proximal processes of the murine dentary. *Dev Dyn* 237(6):1604-1613.